Journal of Orthopaedic Translation 26 (2021) 84–91

Contents lists available at ScienceDirect

Journal of Orthopaedic Translation

journal homepage: www.journals.elsevier.com/journal-of-orthopaedic-translation

Original article

An animal model of early-stage femoral head osteonecrosis induced by cryo-insult in small tailed Han sheep

Cairu Wang [a,b,1], Zhigang Wu [c,d,1], Xiaokang Li [a], Lei Shi [a], Qingyun Xie [b], Da Liu [b], Zheng Guo [a,*], Wei Zheng [b,**]

[a] Department of Orthopaedics, Xijing Hospital, Fourth Military Medical University, Xi'an, Shaanxi 710032, China
[b] Department of Orthopaedics, The General Hospital of Western Theater Command, Chengdu, Sichuan 610083, China
[c] Department of Area Space Hygienics, School of Aerospace Medicine, Air Force Medical University, Xi'an, Shaanxi 710032, China
[d] Department of Orthopaedics, The 63750 Hospital of People's Liberation Army, Xi'an, Shaanxi, 710043, China

ARTICLE INFO

Keywords:
Animal model
Cryo-insult
Femoral Head Osteonecrosis
Sheep

SUMMARY

Purpose: This study investigated the ability of liquid nitrogen cryo-insults to induce early-stage osteonecrosis of the femoral head (ONFH) in small tail Han sheep.
Methods: 16 animals were subjected to unilateral cryo-insult using cryogen equipment with a cryo-insult probe, followed 1, 3, and 6 months later by X-ray, CT scanning, micro-CT scanning, and histological evaluation.
Results: X-ray evaluation of operative femoral heads (Op-FHs) at each time point showed low density areas under the cartilage surface that paralleled sclerosis belts, and CT scans showed sclerosis and cyst areas in Op-FHs. Micro-CT analysis showed that the ratio of bone to total volume and mean trabecular thickness of regions of interest (ROIs) were lower in Op-FHs than in normal femoral heads (No-FHs) at each time point ($n = 4$, $p < 0.05$). Histological evaluation at 1 month showed that necrotic changes were dominant as evidenced by moderate empty lacunae, decreases in the number of hematopoietic cells, and moderate increases in the number of fibroblasts. At 3 and 6 months, fractured trabeculae, fibroblasts, and new blood capillaries were increased, indicating an absorption and repair process. Bone volume fraction of ROIs of Op-FHs was lower than in No-FHs at each time point ($n = 4$, $p < 0.05$) in histological evaluation. At 6 months, the maximum load of No-FHs was higher than Op-FHs ($n = 4$, $p < 0.05$).
Conclusion: These findings indicate that early-stage ONFH can be induced in small tail Han sheep using cryogenic equipment.
The translational potential of this article: This animal model may be helpful in developing new treatment modalities for human ONFH.

Introduction

More than 80% of hips affected by osteonecrosis of the femoral head (ONFH) have been estimated to progress to collapse, requiring hip replacement procedures [1,2]. Treatment of ONFH during early stages may prevent hip collapse. Surgical modalities for early-stage ONFH include core decompression, osteotomy, vascularized or non-vascularized bone substitute implantation, and tantalum rod insertion [1,3]. However, the optimal method has not yet been determined [1,3]. New modalities or substitutes for mechanical support after core decompression procedures are needed. Although in vivo experiments are essential, no ideal models of ONFH have yet been developed in large animals [4,5].

An animal model of ONFH induced by cryogenic insults and progressing to human-like mechanical failure has been described in emus, which are large, exceptionally active bipeds native to Australia [4]. Emus, however, are not conventional experimental animals [4,6], indicating a need to establish models of ONFH in conventional animals, such as sheep and dogs. Methods commonly used to induce bone necrosis include steroid administration [7], ethanol injection [8,9], and cryogenic

* Corresponding author.
** Corresponding author.
E-mail addresses: guozheng@fmmu.edu.cn (Z. Guo), zw770880@126.com (W. Zheng).
[1] These authors contributed equally to this study and are co-first authors.

https://doi.org/10.1016/j.jot.2020.06.004
Received 16 January 2020; Received in revised form 16 June 2020; Accepted 26 June 2020
Available online 28 September 2020

insult [4,6]. OFNH has been induced by corticosteroids in small animals such as rabbit and rats [10,11], but these animals are not suitable for testing surgical modalities in the treatment of ONFH. Ethanol injection and cryogenic insults have shown better ability to induce ONFH in large animals [10,11]. The present study describes a sheep model of ONFH induced by cryogenic insults and its evaluation by imaging and mechanical tests.

Materials and methods

Animals and experimental design

This research was approved by the Institutional Animal Care and Use Committee of the Fourth Military Medical University. 16 adult female small tailed Han sheep, of median age 20 months (range, 16–24 months) and median weight 30 kg (range, 26–35 kg) were raised in two approved sheepfolds in the Experimental Animal Centre of the Fourth Military Medical University. The area of each sheepfold was 25 m^2, allowing animals to move freely.

One femoral head of each animal was selected randomly and subjected to a cryo-insult, with the contralateral femoral head of each animal being a control. After surgery, all the animals were allowed to roam freely in their sheepfold with normal weight bearing. The animals were divided randomly into three groups of four sheep each. At 1, 3, and 6 months, all four animals in each group underwent X-ray examination, CT scanning, micro-CT scanning, and histological evaluation. Besides, another 4 animals were performed with mechanical tests at 6 months (Fig. 1).

Surgical procedures

Before surgical procedures, all the animals performed with X-ray evaluation to verity that the osteoepiphyseal lines of the femoral heads were closed making sure that all animals were skeletal mature. The animals were fasted 24 h before surgery, which was performed in an aseptic animal operating room. The sheep were anesthetized by intramuscular injection of 0.1 ml/kg xylazine hydrochloride (Jilin Huamu Animal Health Product Co. Ltd., China). After shaving and sterilization, a 10 cm incision passing through the greater trochanter was made. The skin, fascia, and muscle layers were separated, and the posterior femoral head–neck juncture was exposed. A foramen (2 mm in diameter and 10 mm in depth) was drilled from the infero-medial aspect of the femoral head–neck junction in the direction of the central femoral head, and liquid nitrogen was sprayed into the foramen using cryogenic equipment (Xinxiang Xinya Cryogenic Vessel Co. Ltd., China; Fig. 2A and B). The femoral heads were frozen for 6 min and thawed with warm saline for 6 min, with the freeze–thaw cycle repeated three times. 450 mL liquid nitrogen was used in each animal. The contralateral femoral heads, which did not undergo surgery, were regarded as controls.

Cefazolin (Cefazolin Sodium For Injection, Sanjing Pharmaceutical Co.,Ltd., 50 mg/kg) was administered intramuscularly at 0.5 h preoperatively and every 8 h for 48 h for prophylactic use. Buprenorphine (Buprenorphine Hydrochloride Injection, TIPR Pharmaceutical Responsible Co., Ltd, 0.01 mg/kg) were administered intramuscularly every 8 h for 3 days for pain management.

X-ray examination

After cryogenic insult, four animals underwent X-ray examinations at each time point (1, 3, and 6 months). Philips Digital Diagnost (Philips, Holland) was used for X-ray evaluation at 70 kV, 1.880 mAs, 1.75 ms, 1.280 dGycm2. Progression of the femurs to femoral head collapse, hip joint arthritis, or femoral neck fracture was evaluated, and areas of sclerosis and low bone density were examined. All evaluations were performed by three radiologists who were blinded to the experimental protocol.

CT scanning

After X-ray examination, the animals were anesthetized by intramuscular injection of 0.1 ml/kg xylazine hydrochloride, followed by CT scanning at each time point. Optima CT660 CT64 (GE MEDICAL SYSTEMS, America) was used for CT scanning, and the parameters were 120 kV in Voltage, 293 mA in Current. The raw data, in DICOM format, were imported into MIMICS 16.0 software (Materialise, Belgium). This software was used to evaluate the appearance of sclerosis, cysts, and articular surface collapse evaluated slice-by-slice. All evaluations were performed by three radiologists blinded to the experimental protocol.

Micro-CT scanning

At each time point (1, 3, and 6 months), four animals were sacrificed, and their femoral heads were collected and immediately fixed in 10% formalin for 72 h. The specimens were subjected to micro-CT scanning using the Y. Cheetah system (YXLON, Germany), with scans at 1, 3 and 6 months performed at 80 kV, 500 μA, and a spatial resolution of 30 μm. The acquired data, in DICOM format, were processed using VGStudio MAX 2.1 software. A cylindrical region of interest (ROI), 10 mm in diameter and 6 mm in height, was selected in the upper-medial aspect of each femoral head, such that the central axes of the ROIs and the femoral necks were aligned. The top surface of the cylinder was tangential to the fovea of the femoral heads, and the surface of the cylinder was tangential to the epiphyseal line of the femoral heads (Fig. 3). Bone volume to total volume (BV/TV), mean trabecular thickness (Tb.Th), and mean trabecular number (Tb.N) in ROIs were calculated and reported as mean ± standard deviation. These parameters were quantitatively analyzed in each group.

Histological examination

The fixed femoral heads were decalcified in EDTA solution for 2–3 weeks and cut coronally into two equal parts. The specimens were dehydrated, embedded in paraffin, cut into 5 μm slices, and stained with hematoxylin-sosin (H-E). An area measuring 10 × 6 mm in the inner-upper part of the femoral head, which coincided with ROI of micro-CT scanning, was selected as the ROI and examined under a light microscope. Image-Pro Plus software (Silver Spring, MD, USA) was used to calculate the bone volume fraction, which was defined as the ratio of bone tissue to total area.

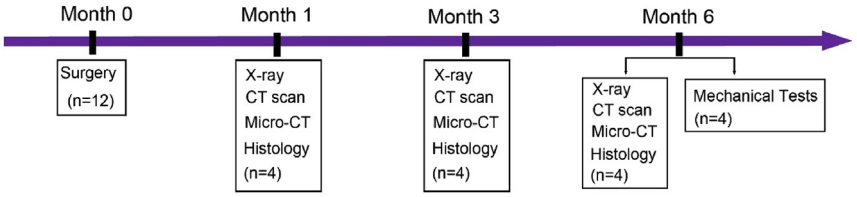

Figure 1. Schematic illustration of the experimental design.

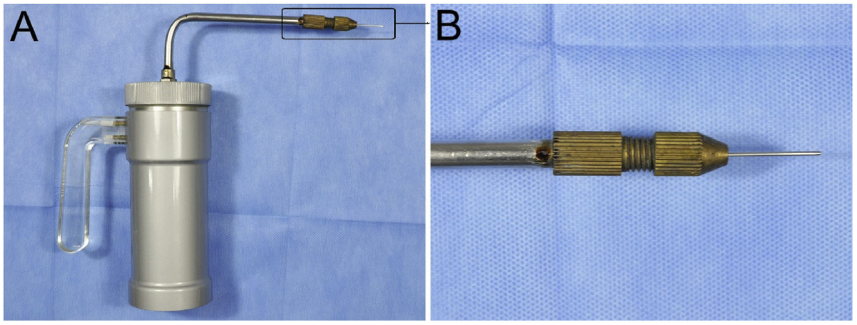

Figure 2. Illustrations of the cryogenic equipment (A) and the cryo-insult probe (B).

Mechanical tests

At 6 months, another 4 animals were sacrificed, and the femurs were harvested and stored at −80 centigrade. The testing process was similar with previous reports [12,13]. Briefly, using a self-designed clamping apparatus, the proximal femurs were fixed on a universal mechanical testing machine (AGS 10 KNG, SHIMADZU, Japan). A vertical lord with a speed of 2 mm/Min was applied to each femoral head. Load and displacement data were documented and analyzed.

Statistical analysis

All quantitative parameters in experimental and control lateral femoral heads, including BV/TV, Tb.Th, Tb.N, and Tb.Sp in ROIs of micro-CT scans, and percentage of empty lacunae in histologically determined ROIs were quantitatively compared using SPSS 16.0 software (IBM Corp., USA). A p-value <0.05 was considered statistically significant.

Results

Each animal showed good mental status and ate regularly after surgery. The operative wounds healed on time, with no evidence of sudation or maturation. All animals were unable to walk normally immediately and for 1–2 weeks after the operation. Although these animals healed thereafter, they were again unable to walk normally 5–6 weeks after the operation. None of these animals died suddenly or became bedridden throughout the study period.

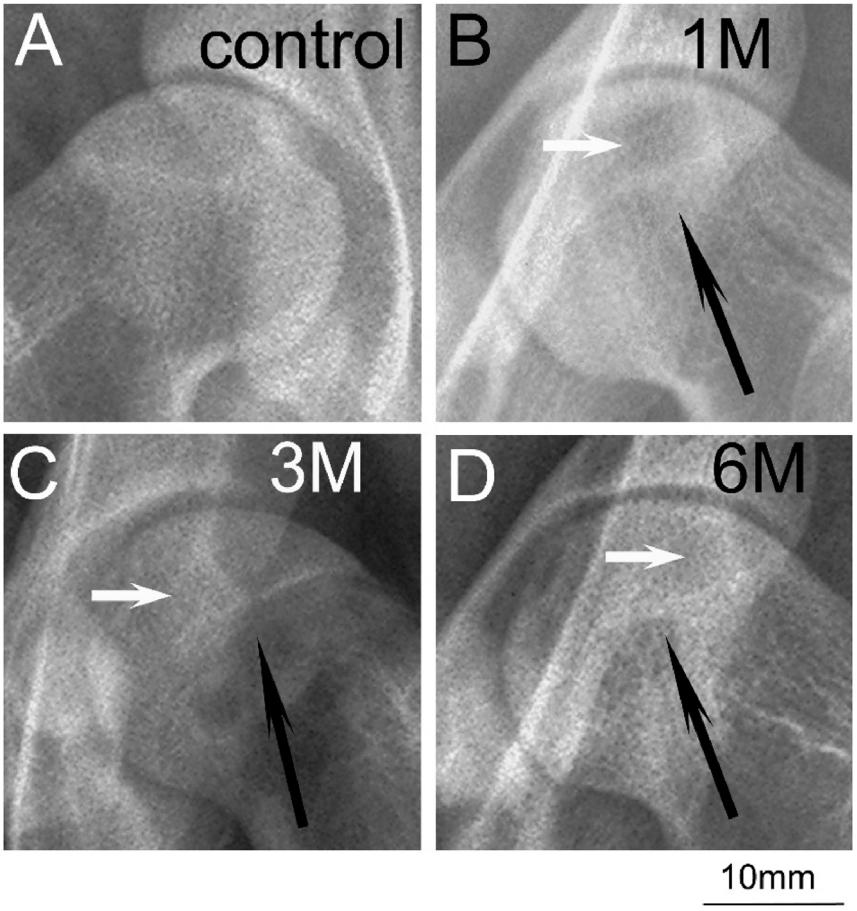

Figure 3. X-ray images. (A) Control femoral heads. (B–D) Operated femoral heads at 1 month (B), 3 months (C), and 6 months (D). White arrows indicate low density areas, and black arrows indicate cryo-insult channels.

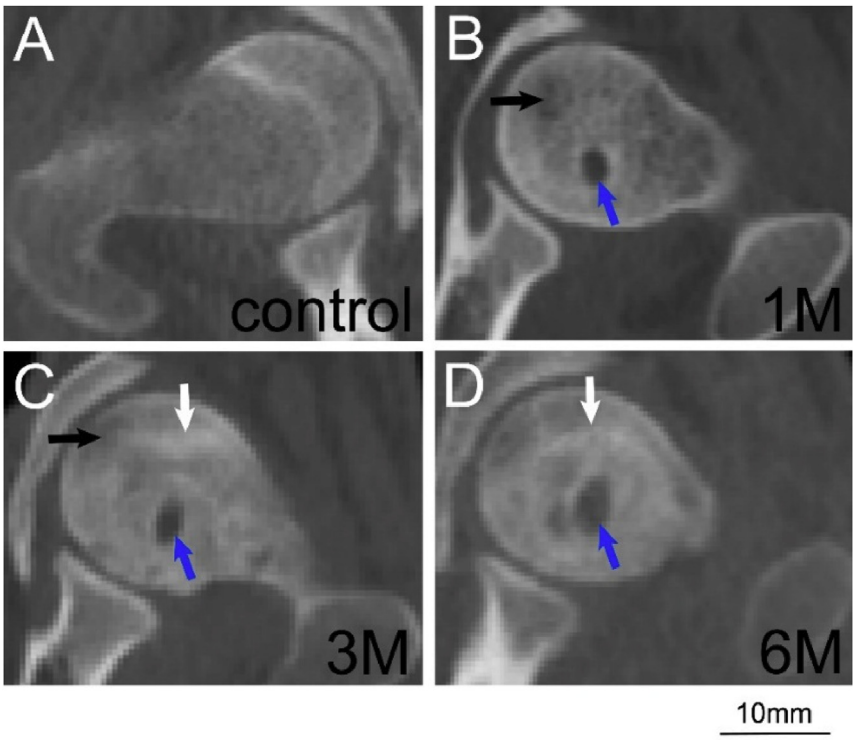

Figure 4. Cross sectional views of femoral heads on CT scans. (A) Control femoral heads. (B–D) Operated femoral heads at 1 month (B), 3 months (C), and 6 months (D). White arrows indicate areas of sclerosis, black arrows indicate cysts, and blue arrows indicate cryo-insult channels. (For interpretation of the references to colour in this figure legend, the reader is referred to the Web version of this article.)

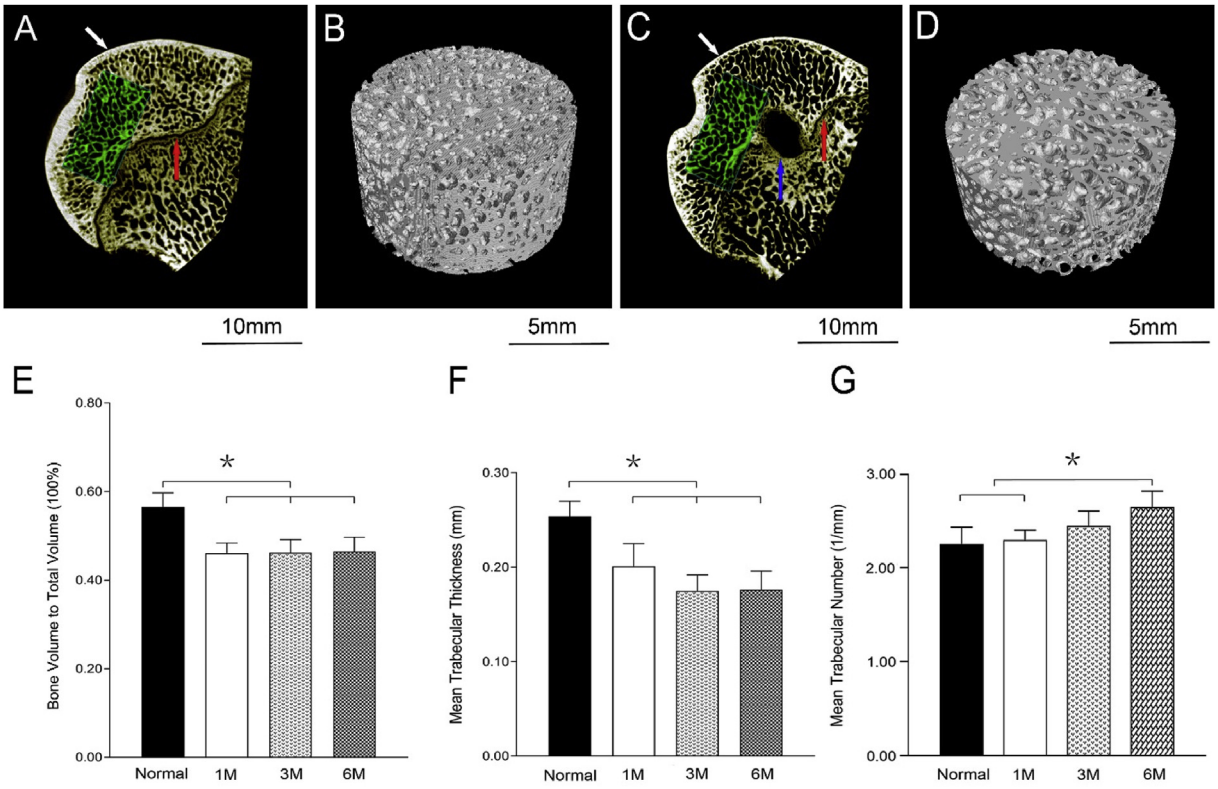

Figure 5. Mesial coronal section images of the femoral heads on micro-CT scans. A and B: Control femoral heads. C and D: Femoral heads of sheep sacrificed after 3 months. Green areas are ROIs, red arrows indicate epiphyseal lines, blue arrows indicate channels of cryo-insults, and white arrows indicate articular surfaces. Comparisons of BV/TV (E), Tb.Th (F), and Tb.N (G) of ROIs of control femoral heads and of operated femoral heads after 1, 3, and 6 months. Asterisks (*) indicate statistical significance ($p < 0.05$, n = 4). (For interpretation of the references to colour in this figure legend, the reader is referred to the Web version of this article.)

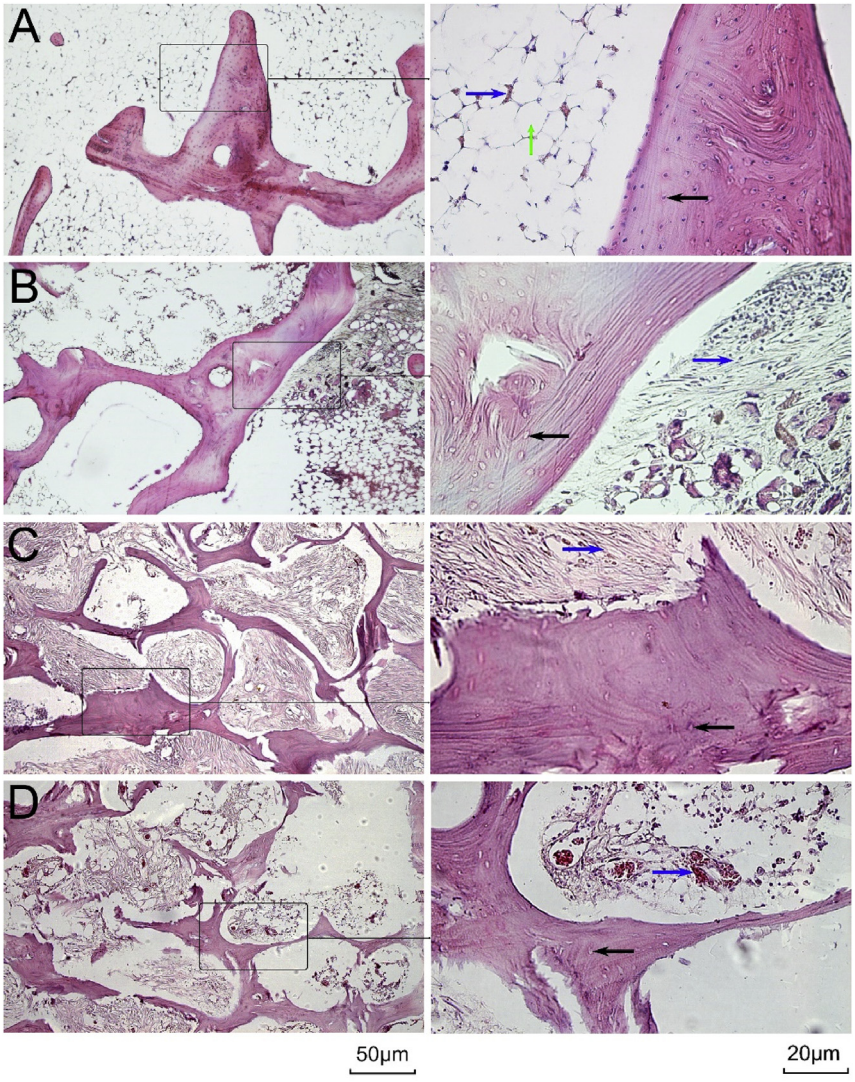

Figure 6. Histological images of the femoral heads (hematoxylin-eosin dyeing). (A) Control femoral heads. The black arrow indicates bone lacunae filled with osteocytes; the blue arrow indicates hematopoietic cells; and the green arrow indicates lipocytes. (B–D) Femoral heads 1 (B), 3 (C), and 6 (D) months after cryo-insult. The black arrows indicate empty bone lacunae. The blue arrows in B and C indicate fibroblasts, whereas the blue arrow in D indicates new blood capillaries. (For interpretation of the references to colour in this figure legend, the reader is referred to the Web version of this article.)

X-ray evaluation

During all the observing period, none of the femoral heads underwent cryo-insult progress to collapse, hip joint arthritis, and femoral neck fracture, but they showed differences in the extent of inhomogeneous changes. Some showed low density areas under the cartilage surface that ran parallel with sclerosis belts (Fig. 3B–D, white arrows). The hip joint space in operated femoral heads remained normal, with no indications of osteoarthritis. Until 6 months, the cryo-insult channel (Fig. 3B–D, black arrow) remained open, indicating a slow recovery process.

CT scan

None of the control femoral heads showed evidence of sclerosis or cyst areas at any time point. Operated femoral heads, however, showed areas of sclerosis (Fig. 4B–D, white arrows) and cysts (Fig. 4B–D, black arrows). Until 6 months, the freezing tunnels did not heal (Fig. 4B–D, blue arrows), indicating that the healing process was slow in necrotic femoral heads. None of the operated hip joints showed evidence of severe hip arthritis or femoral head collapse, with all having normal joint space.

Micro-CT scan

Mesial coronal section images of micro-CT scans showed that, comparing with the normal femoral head (Fig. 5A and B), the trabeculae and cartilage of intervened femoral head (Fig. 5C and D, white arrows) became thinner after cryo-insults, and that the cryo-insult channels (Fig. 5C, blue arrows) were not closed until 6 months after the operation, indicating a slow recovery process. BV/TV ratios of ROIs of control and operated femoral heads at 1, 3, and 6 months were 0.565 ± 0.032, 0.461 ± 0.023, 0.462 ± 0.030, and 0.465 ± 0.032, respectively, with all differences between operated and control femoral heads being statistically significant (Fig. 5E; $n = 4$, $p < 0.05$). The Tb.Th of ROIs of control and operated femoral heads at 1, 3, and 6 months were 0.254 ± 0.016, 0.201 ± 0.024, 0.175 ± 0.017, and 0.176 ± 0.020, respectively, with all differences between operated and control femoral heads being statistically significant (Fig. 5F; $n = 4$, $p < 0.05$). The Tb.N of ROIs of control and operated femoral heads at 1, 3, and 6 months were 2.258 ± 0.177, 2.304 ± 0.102, 2.453 ± 0.155, and 2.652 ± 0.170, respectively, with the Tb.N of ROIs of operated femoral heads at 6 months being significantly higher than the Tb.N of ROIs of control and of operated femoral heads at 1 month (Fig. 5G; $n = 4$, $p < 0.05$). Higher Tb.N of ROIs at 6 months suggested a greater number of new bone trabeculae.

Histological examination

Histological examination of control femoral heads showed that bone trabeculae were intact and no fractured bone was present. The bone lacunae were filled with osteocyte nuclei, which were dyed to navy blue (Fig. 6A, black arrow). Abundant hematopoietic cells (Fig. 6A, blue

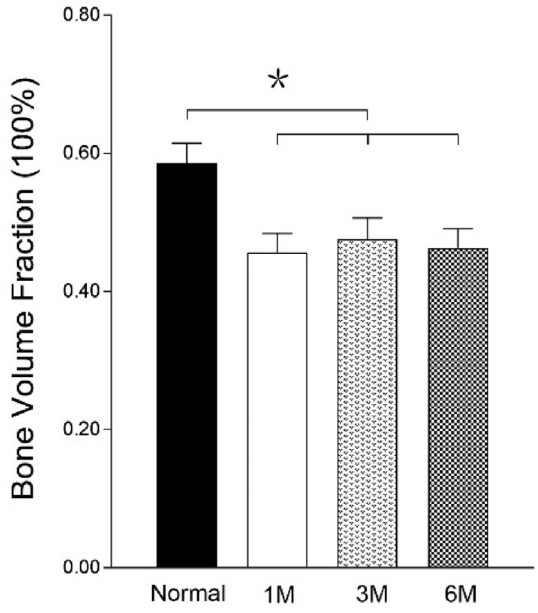

Figure 7. Bone volume fraction of ROIs in four groups. Asterisks (*) indicate statistical significance ($p < 0.05$, n = 4).

arrow) and lipocytes (Fig. 6A, green arrow) were observed in the medullary cavity of cancellous bone. The cells filled in bone marrow (Fig. 6A) were hematopoietic cells and fat cells. Based on previous report [14], the large, round and bubble-like cells were fat cells, and the dark-stained cells between the fat cells were hematopoietic cells in H&E staining. At 1 month after cryo-insults, most osteocyte nuclei in bone lacunae disappeared, with the bone lacunae becoming empty (Fig. 6B, black arrow). The numbers of hematopoietic cells and lipocytes decreased, whereas fibroblasts (Fig. 6B, blue arrow) began to appear in the medullary cavity. At 3 months, the trabeculae became fractured (Fig. 6C), and the number of fibroblasts increased (Fig. 6C, blue arrow). At 6 months, the fractured trabeculae became absorbed (Fig. 6D), and some new blood capillaries began to appear in the medullary cavity. Whereas, there was seldom capillary in ROI of control group, 1 and 3 month groups (Fig. 6A, B and C), which was similar with previous reports [7,15,16].

Bone volume fraction of control and operated femoral heads at 1, 3, and 6 months were 0.586 ± 0.029, 0.457 ± 0.027, 0.476 ± 0.031, and 0.463 ± 0.028, respectively, with all differences between operated and control femoral heads being statistically significant (Fig. 7, n = 4, $p <$ 0.05).

Mechanical tests

All the specimens did not show any femoral head collapse instead of femoral head-neck juncture fracture. The maximum loads of normal and necrotic femoral heads were 3521.52 ± 309.26 N and 2964.50 ± 289.35 N, which had a statistical significance (Fig. 8, n = 4, $p < 0.05$).

Discussion

After standard core decompression, early-stage necrotic femoral heads often lose their mechanical strut and likely progress to collapse; these patients will likely require total hip arthroplasty. Substitutes selected as mechanical support materials for subchondral bones after core decompression procedures include vascularized and non-vascularized bone-grafts and tantalum rods. Bone graft transplantation is frequently a complicated surgical procedure, requiring prolonged hospitalization and with a high risk of complications [1]. Tantalum rods have a lower survival rate on middle and long follow-up, and histopathologic retrieval analysis showed poor bone ingrowth into these rods [17,18]. Effective substitutes are needed urgently, with experiments in large animals required for preclinical testing. To date, however, no ideal model of early-stage ONFN has been developed in large animals, such as sheep and dogs, which are species commonly used for in vivo experiments.

An animal model of ONFH was developed in emus [4,6]. Due to the special biomechanical environment of the hip joint in these bipeds and their exceptional level of activity, this model can progress to femoral head collapse. However, emus are large, ostrich-like flightless birds native to Australia and are not used as a traditional animal model for musculoskeletal experiments. Sheep and dogs are large quadrupeds, frequently used as experimental animals, making them especially suitable for the development of new bone substitutes. Several studies have described animal models of early-stage ONFH in sheep and canines [8,9,14,16]. One study [9] described a model of early-stage ONFH induced by absolute ethanol injection in merino sheep, a type not usually available in China.

Small tailed Han sheep are pure bred animals with similar figure size and good disease tolerance, which are frequently used as in vivo models in China [19–21]. The sheep used in this experiment had a median age of 20 months (range, 16–24 months). When the small tailed Han sheep grows over the age of 14 months, they become sexual maturity and begin to give birth to little sheep. Thus, the animals selected in this study were skeletal mature sheep. To verify this, each animal performed with X-ray evaluation before surgical procedures. Our preliminary study investigated the feasibility of inducing femoral head necrosis in these sheep by injection of absolute ethanol, which method was also used in previous reports [8,9]. We found that most of the ethanol infiltrated into the femoral medullary cavity through the femoral neck, with little ethanol penetrating into the femoral head. Histological examination and micro-CT scanning of normal femoral heads in small tailed Han sheep suggested that the findings observed after injection of absolute ethanol were related to the special array of cancellous bone in the femoral head and neck of these animals. Cancellous bone from the femoral neck to the femoral head gradually thickens, inhibiting the penetration of absolute ethanol. These findings suggested that the ability of absolute ethanol to induce necrosis is limited.

Another feasible method of inducing ONFH in large animals is through cryo-insult of liquid nitrogen [4,10,11,14]. Osteonecrosis can be induced in a dog model of ONFH by covering the femoral head with rubber tubing and pouring liquid nitrogen into the tube [22]. ONFH can also be induced in dogs by coiling a rubber tube around the femoral neck and circulating liquid nitrogen through the tube [16]. Radiography showed lytic areas at the femoral head and neck and dense bone near the base of the femoral neck. These methods usually induced extensive necrotic areas, including the subchondral bone, femoral head and neck, and even the cartilage of the articular surface, making this model unsuitable for testing treatment modalities for early-stage ONFH. The

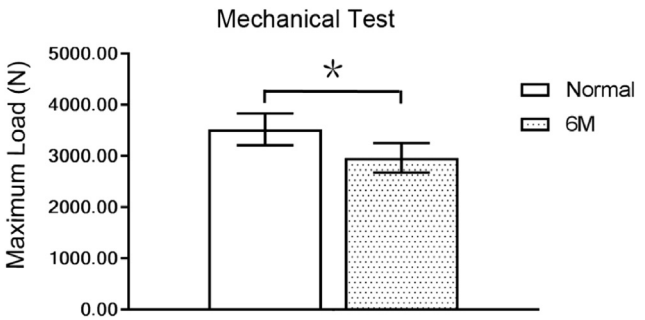

Figure 8. The maximum loads in mechanical tests. Asterisks (*) indicate statistical significance ($p < 0.05$, n = 4).

femoral head of an ideal animal model of ONFH should have necrotic areas analogous to those of humans. Moreover, the ideal animal model should involve the induction of a uniform lesion with anatomic proximity to the articular surface and anatomic continuity with adjacent viable bone [10]. In emus, the introduction of a cryo-probe to deliver liquid nitrogen resulted in the successful establishment of an ONFH model [4,6].

In this study, ONFH was induced in small tailed Han sheep using cryogenic equipment with a cryo-insult probe, similar to the method used to induce ONFH in emus [4,6]. The feasibility and effectiveness of this model were investigated by X-ray and CT imaging and by micro-CT and histological examination. ONFH is believed to be a multifactorial diseases. These risk factors include corticoid administration, alcohol intake, smoking, and other chronic diseases [23]. No matter what the underlying cause is, all forms of ONFH are related to blood flow impairment [24]. The extreme cold can cause rupture of cellular membranes as a result of crystallization, dehydration, and toxic concentration of electrolytes due to removal of water form solution, liquid protein damage within the cell membranes, and vascular stasis. The integrity of the intraosseous vessels often destroyed in aforementioned process [16]. This animal model as well as human ONFH caused by aforementioned risk factors have a similar pathogenesis that the blood flow are impaired.

The aim of this study was to establish a sophisticated animal model of early-stage ONFH in small tailed Han sheep that would enable the testing of new treatment modalities. X-ray examination showed low density areas under the cartilage surface and paralleling sclerosis belts, changes typical of early-stage ONFH in humans. Researchers often define pre-collapsed femoral head as early-stage ONFH, and collapsed femoral head as late/end-stage ONFH [4,25,26]. ONFH classification systems, such as Steinberg or Association Research Circulation Osseous (ARCO), can be available for this animal model. In this animal model, the femoral head did not progress to collapse and showed sclerosis belts in X-ray and CT scan. Thus, ONFH in this model could be classified as stage II in Steinberg or ARCO classification system. CT scanning showed the development of areas of sclerosis and cysts over time after freezing intervention. Micro-CT analysis showed that the BV/TV ratio and the mean Tb.Th in ROIs were lower in treated than in normal femoral heads, suggesting necrosis and the absorption of cancellous bone. Furthermore, the Tb.N of ROIs was higher in treated femoral heads at 6 months than in normal femoral heads and in treated femoral heads at 1 month, indicating a slow bone repair process after the cryo-insult. Moreover, X-rays and CT scans showed that the freezing tunnels did not heal until 6 months after the intervention, again suggesting a slow repair process.

Histological evaluation is regarded as the gold standard for diagnosing osteonecrosis. Typical changes include empty lacunae, fractured trabeculae, decreased numbers of hematopoietic cells and lipocytes, and increased numbers of fibroblasts and newly formed blood capillaries [27]. All of these changes were observed in this model. This finding suggested that the necrotic trabeculae in the ROIs of treated femoral heads did not heal during the entire observation period. These necrotic trabeculae became fractured and were absorbed at 3 and 6 months, as verified histologically. The mechanical strut of these necrotic trabeculae was decreased, a finding that suggested the mechanism of femoral head collapse in humans. The repair process could also be assessed histologically because newly formed blood capillaries accompanied by increased numbers of fibroblasts were observed at 6 months. However, we did not observe newly formed immature woven bone deposited on dead trabecular bone or the process of creeping substitution.

We did not observe evidence of femoral head collapse in this model throughout the entire observation period. This may be attributed to differences in the mechanical environments of quadrupeds and humans [4,10] or to the short duration of cryo-insult time. The parameters of cryo-insult used in this study, including the duration of exposure and the number and duration of freeze–thaw cycles, were based on previous reports [4,6]. Although one small-sized small tailed Han sheep experienced femoral head collapse in our preliminary study, none of the sheep experienced femoral head collapse in the present study. Thus, this model can be classified as stage Ior II in Steinberg or ARCO classification systems.

There were total 12 femoral heads left untreated. We randomly selected 4 of them as control group. The animals selected in this study were 16–24 months old, which were skeletal mature and verified by X-ray examination before the surgery. For skeletal mature human being or experimental animals, the growth itself can seldom affect the process of femoral head osteonecrosis [1,10]. Thus, as long as the animal was skeletal mature, the femoral head left untreated can be selected as control. 4 animals randomly selected could stand for all the normal femoral heads.

One limitation of this study was that the observation period was only 6 months, preventing a determination of whether the treated femoral heads would later progress to collapse. Additional studies are also required to further investigate the repair process of new bone deposition and creep substitution. Another limitation of this study is that there were only 4 animals in each group. The power of statistical analysis was too low. But, the animal number should be as little as possible to fulfill the ethical principle of Reduction. In the process of experimental design, we had consulted statisticians and referenced previous similar studies. Finally, we determined that 16 animals were used in this study. The other limitation was that we just observed vessel changes in the images without quantitative analysis. In the following study, we will use other method to test mciroangiography.

Conclusion

Early-stage ONFH can be successfully induced in small tailed Han sheep using cryogenic equipment with a cryo-insult probe. This model may help in the development of new treatment modalities for early-stage ONFH in humans.

Conflict of Interest

The authors have no conflicts of interest to disclose in relation to this article.

Acknowledgments

This work was supported by the National Key R&D Program of China (2017YFC1104900), the National Natural Science Foundation of China (No. 81171773 and No. 5150010028), and the Projects of Science and Technology of Sichuan Province (No. 2019YFS0122).

References

[1] Mont MA, Cherian JJ, Sierra RJ, Jones LC, Lieberman JR. Nontraumatic osteonecrosis of the femoral head: where do we stand today?: a ten-year update. J Bone Joint Surg 2015;97:1604–27.
[2] Mont MA, Zywiel MG, Marker DR, McGrath MS, Delanois RE. The natural history of untreated asymptomatic osteonecrosis of the femoral head: a systematic literature review. J Bone Jt Surg Am 2010;92:2165–70.
[3] Chughtai M, Piuzzi NS, Khlopas A, Jones LC, Goodman SB, Mont MA. An evidence-based guide to the treatment of osteonecrosis of the femoral head. Bone Jt J 2017;99-B:1267.
[4] Conzemius MG, Brown TD, Zhang Y, Robinson RA. A new animal model of femoral head osteonecrosis: one that progresses to human-like mechanical failure. J Orthop Res 2002;20:303–9.
[5] Zheng LZ, Liu Z, Lei M, Peng J, He YX, Xie XH, et al. Steroid-associated hip joint collapse in bipedal emus. PLoS One 2013;8:e76797.
[6] Reed KL, Brown TD, Conzemius MG. Focal cryogen insults for inducing segmental osteonecrosis: computational and experimental assessments of thermal fields. J Biomech 2003;36:1317–26.
[7] Qin L, Zhang G, Sheng H, Yeung K, Yeung H, Chan C, et al. Multiple bioimaging modalities in evaluation of an experimental osteonecrosis induced by a combination of lipopolysaccharide and methylprednisolone. Bone 2006;39:863–71.
[8] Wang C, Wang J, Zhang Y, Yuan C, Liu D, Pei Y, et al. A canine model of femoral head osteonecrosis induced by an ethanol injection navigated by a novel template. Int J Med Sci 2013;10:1451–8.

[9] Manggold J, Sergi C, Becker K, Lukoschek M, Simank HG. A new animal model of femoral head necrosis induced by intraosseous injection of ethanol. Lab Anim 2002; 36:173–80.
[10] Conzemius MG, Brown TD. Animal models of osteonecrosis. Tech Orthop 2001;16: 90–7.
[11] Jones LC, Allen MR. Animal models of osteonecrosis. Clin Rev Bone Miner Metabol 2011;9:63–80.
[12] Wang C, Liu D, Xie Q, Liu J, Deng S, Gong K, et al. A 3D printed porous titanium alloy rod with diamond crystal lattice for treatment of the early-stage femoral head osteonecrosis in sheep. Int J Med Sci 2019;16:486–93.
[13] Wang C, Xie Q, Yang L, Liu J, Liu D, Li Z, et al. A 3D printed porous titanium alloy rod with biogenic lamellar configuration for treatment of the early-stage femoral head osteonecrosis in sheep. J Mech Behavior Biomed Mater 2020;106:103738.
[14] Velez R, Soldado F, Hernandez A, Barber I, Aguirre M. A new preclinical femoral head osteonecrosis model in sheep. Arch Orthop Trauma Surg 2011;131:5–9.
[15] Nishino M, Matsumoto T, Nakamura T, Tomita K. Pathological and hemodynamic study in a new model of femoral head necrosis following traumatic dislocation. Arch Orthop Trauma Surg 1997;116:259–62.
[16] Malizos KN, Quarles LD, Seaber AV, Rizk WS, Urbaniak JR. An experimental canine model of osteonecrosis: characterization of the repair process. J Orthop Res 1993; 11:350–7.
[17] Tanzer M, Bobyn JD, Krygier JJ, Karabasz D. Histopathologic retrieval analysis of clinically failed porous tantalum osteonecrosis implants. J Bone Jt Surg Am 2008; 90:1282–9.
[18] Veillette CJ, Mehdian H, Schemitsch EH, McKee MD. Survivorship analysis and radiographic outcome following tantalum rod insertion for osteonecrosis of the femoral head. J Bone Jt Surg Am 2006;88(Suppl 3):48–55.
[19] Li X, Gao P, Wan P, Pei Y, Shi L, Fan B, et al. Novel bio-functional magnesium coating on porous Ti6Al4V orthopaedic implants:in vitroandIn vivoStudy. Sci Rep 2017;7:40755.
[20] Li Y, Wu ZG, Li XK, Guo Z, Wu SH, Zhang YQ, et al. A polycaprolactone-tricalcium phosphate composite scaffold as an autograft-free spinal fusion cage in a sheep model. Biomaterials 2014;35:5647–59.
[21] Wu SH, Li Y, Zhang YQ, Li XK, Yuan CF, Hao YL, et al. Porous titanium-6 aluminum-4 vanadium cage has better osseointegration and less micromotion than a poly-ether-ether-ketone cage in sheep vertebral fusion. Artif Organs 2013;37:E191–201.
[22] Takaoka K, Yoshioka T, Hosoya T, Ono K, Takase T. The repair process in experimentally induced avascular necrosis of the femoral head in dogs. Arch Orthop Trauma Surg 1981;99:109–15.
[23] Mont MA, Jones LC, Hungerford DS. Nontraumatic osteonecrosis of the femoral head: ten years later. J Bone Jt Surg Am 2006;88:1117–32.
[24] Petek D, Hannouche D, Suva D. Osteonecrosis of the femoral head: pathophysiology and current concepts of treatment. EFORT Open Rev 2019;4:85–97.
[25] Utsunomiya T, Motomura G, Ikemura S, Kubo Y, Sonoda K, Hatanaka H, et al. Effects of sclerotic changes on stress concentration in early-stage osteonecrosis: a patient-specific, 3D finite element analysis. J Orthop Res 2018;36:3169–77.
[26] Zhao DW, Yu XB. Core decompression treatment of early-stage osteonecrosis of femoral head resulted from venous stasis or artery blood supply insufficiency. J Surg Res 2015;194:614–21.
[27] Seamon J, Keller T, Saleh J, Cui Q. The pathogenesis of nontraumatic osteonecrosis. Arthritis 2012;2012:601763.